PHYSICAL REVIEW B VOLUME 23, NUMBER 4 15 FEBRUARY 1981

Screening of hot-carrier relaxation in highly photoexcited semiconductors

Ellen J. Yoffa
IBM Thomas J. Watson Research Center, Yorktown Heights, New York 10598
(Received 2 September 1980)

The carrier density dependence of the hot-carrier energy relaxation rate in highly photoexcited semiconductors is investigated. Results of these calculations indicate important differences between polar direct-gap and nonpolar indirect-gap materials. The critical carrier density (N_c) for the onset of screening in polar semiconductors is found to increase with both effective mass and phonon energy. A method for predicting trends among these materials with respect to N_c is briefly described. Calculations for GaAs predict that the hot-carrier cooling rate begins to decrease at $N_c \approx 6\times 10^{16}$ cm^{-3}. Above this density the phonon emission frequency falls rapidly. In contrast, the effects of screening in Si are shown to be negligible for $N \lesssim 10^{19}$ cm^{-3}. In this case, a significant reduction in the energy relaxation rate does not occur until $N \sim 10^{21}$ cm^{-3}.

I. INTRODUCTION

Recently there has been widespread interest in the use of high-intensity pulsed lasers to transfer energy to semiconductor surfaces by means of rapid carrier generation. For these experiments, it is necessary to understand not only the resultant flow of heat through the lattice but also the manner in which the energy is transferred from the laser to the semiconductor lattice. This paper investigates the carrier density dependence of the rate of phonon emission by a plasma of hot electrons and holes in semiconductors highly excited by laser irradiation. In a previous paper,[1] such considerations were confined to the example of Si during pulsed laser annealing. These experiments typically involve ~10-ns laser pulses of power 10^8 W/cm^2 (total energy density of ~1 J/cm^2).[2,3] In such a situation, the carrier dynamics must be investigated before the heat flow can be adequately described.[1,4–6] It was shown[1] that the laser is not strongly coupled to the lattice directly through the phonons but is instead initially absorbed by the carrier system (through electron-hole pair creation and free-carrier absorption) with negligible accompanying loss of energy to the lattice. The details of phonon emission depend on the configurations in energy and space of the carriers at the time emission occurs. Consequently, it is important to understand how the carriers redistribute following excitation.

The previous analysis is here extended to apply to another class of experiments, in which semiconductors (e.g., GaAs and Ge) are pumped by laser pulses at energy densities ~10^{-6}–10^{-2} J/cm^2 and subsequent probe pulse absorption,[7–11] reflectivity,[12] or luminescence[13] is monitored. Calculations in this paper predict important differences between polar direct-gap and nonpolar indirect-gap semiconductors in the carrier density dependence of the hot-carrier relaxation rate. The critical carrier density for the onset of screening in polar direct-gap semiconductors is found to increase with both effective mass and phonon energy. This result can be used to predict *trends* among these semiconductors with respect to the density required to decrease the hot-carrier energy relaxation rate. For the specific example of GaAs, it is shown that a reduction in the rate of phonon emission first occurs at an easily attainable carrier density, $N \approx 6\times 10^{16}$ cm^{-3}. By $N \sim 10^{18}$ cm^{-3}, the intravalley transitions are screened and the cooling rate falls very rapidly to a value appropriate to emission of intervalley phonons. In contrast, screening of the energy relaxation rate in Si is negligible at densities less than $N \sim 10^{19}$ cm^{-3} and a significant reduction in this rate does not occur until $N \sim 10^{21}$ cm^{-3}.

The redistribution of carriers in energy and space that takes place prior to and simultaneously with phonon emission is discussed in the rest of this section. In Sec. II the author's previous calculation[1] of the effect of a dense plasma of hot carriers on the phonon emission frequency in a semiconductor is generalized to include transitions between inequivalent valleys. In Sec. III critical carrier densities for effective screening in Si and GaAs are calculated and the density dependence of phonon emission rates is examined. A comparison of the two types of semiconductor appears in Sec. IV. A method for predicting the ordering of semiconductors with respect to critical densities for the onset of screening is described.

Laser excitation does not instantaneously generate equilibrium carrier distributions. At sufficiently high carrier densities thermalization processes are such that the energy largely remains within the system of carriers,[14] i.e., rapid collisions among carriers dominate carrier-lattice collisions and the carriers equilibrate among themselves before they thermalize with the lattice. Evidence that such a circumstance is

physically realizable is that whereas certain radiative recombination intensities oscillate with excitation photoenergy at lower rates of laser excitation (for which $N \sim 10^{11}-10^{14}$ cm^{-3}),[15] they do not exhibit such behavior at higher laser intensities (where N is much larger).[16,17] Shah and Leite[18] have shown that a highly excited electron gives a fraction $N/(N+N_c^*)$ of its excess energy to the electron gas. For GaAs, they calculated the critical density N_c^* to be $N_c^* \approx 7\times 10^{17}$ cm^{-3}. Interactions involving carriers alone occur on a time scale on the order of the inverse plasma frequency, which for carrier densities of $\sim 10^{17}$ cm^{-3} in Si and GaAs is roughly 10^{-13} s and varies as $N^{-1/2}$. Shank *et al.*, using a time-resolved absorption technique,[10] have determined that the time for emission of polar LO phonons by photoexcited carriers in GaAs is less than a few tenths of a picosecond. A similar experimental technique has been used[8,19] to determine that phonon emission times in Ge are roughly on the order of 10^{-12} s.

As long as the carrier collision rates exceed the appropriate phonon emission rates, a carrier temperature can be defined. This paper deals with the very-high-density regime[20] in which carrier collisions lead to electron and hole distribution functions characterized by distinct electron and hole quasi-Fermi levels and a common carrier temperature which greatly exceeds the lattice temperature.

Although at low carrier densities in Si the energy leaves the system of carriers during recombination (e.g., recombination at traps), at sufficiently high densities the dominance of Auger processes insures that the energy lost from the carriers is a negligible fraction of their total energy. Instead, the pair recombination energy is picked up as kinetic energy by a third carrier, which then rapidly equilibrates with the rest of the carriers in the manner described above. This process is driven by the excess density of electrons and holes over that which would exist at equilibrium at the carrier temperature established by carrier thermalization. In a direct-gap semiconductor such as GaAs, radiative channels dominate recombination until much higher carrier densities than in an indirect-gap material like Si. Nevertheless, because the calculations presented in this paper apply to the case of rapid carrier thermalization, the results are in general independent of the dominant mode of recombination. The specific recombination mechanism enters only in determination of the quasi-Fermi level positions and in governing the dependence in steady state of the carrier temperature on the input laser energy.

In recent experimental investigations of hot-carrier relaxation in GaAs,[10–13,17,18] the total energy contained in the laser pulse cannot significantly heat the lattice. Nevertheless, the incident power is sufficiently high to generate carriers to densities at which screening effects are expected to occur. Using time-resolved near-band-gap transmission measurements, Leheny *et al.*[17] inferred the initial hot-carrier cooling rate to be independent of carrier density at moderate densities, $N < 5\times 10^{17}$ cm^{-3}. However, for densities exceeding that value, they found a significant slowing down of the initial rate at which the carrier temperature cools to the lattice temperature. In addition, for $N > 10^{18}$ cm^{-3}, the carriers cannot be described in terms of a thermalized distribution, an effect which they could not attribute to screening of the carrier-phonon interaction.[13,17]

Ehrenreich[21] has calculated the effect of high carrier densities on carrier transport in heavily doped polar semiconductors in which carrier–optical-phonon scattering has a large influence on the mobility. He found that screening effects grow in importance when the plasma frequency exceeds the phonon frequency, especially at low temperatures. He suggested that the resultant reduction in carrier-phonon coupling (this interaction being the primary energy-loss and heat dissipation mechanism) could cause the carriers to heat up more rapidly under the influence of strong electric fields than at lower carrier densities in the absence of screening.

Of course, carrier diffusion is simultaneous with energy redistribution.[22–24] The diffusion process is not a simple one: whereas carrier energy is a conserved quantity under steady-state conditions, the carrier number is not. When carriers diffuse from the surface, they take their energy with them leaving an altered density of energy and carriers. There is no *a priori* reason for these resulting quantities to be in equilibrium with each other, and if they are not, rapid recombination (or ionization) will take place in order to restore equilibrium in the remaining volume. The diffusion is characterized by an ambipolar diffusion coefficient which is a function of the carrier temperature and may consequently be large. Although the energy is absorbed into the carrier system in an absorption depth δ, as a result of the diffusion the energy will be given to the lattice by the carriers in a depth which exceeds δ and, for rapid enough diffusion and high enough laser frequency, may be determined primarily by α.[22,25] α here is the effective energy diffusion length of the hot carriers, that is, the distance a carrier can diffuse before it loses its identity as a hot carrier.

II. PHONON EMISSION

The phonon emission rate is related directly to the carrier excitation spectrum, which is

$$\mathrm{Im}\frac{1}{\epsilon(\tilde{q},\omega)} = \frac{\epsilon_2}{\epsilon_1^2+\epsilon_2^2}\ , \tag{1}$$

where ϵ_1 and ϵ_2 are the real and imaginary parts of the complex dielectric function $\epsilon(\tilde{q},\omega)$. Within the

random-phase approximation,[26]

$$\epsilon_2(\tilde{q},\omega)=\frac{4\pi^2e^2}{\Omega q^2}\sum_{ij}\sum_{\tilde{k}\sigma}f^i_{\tilde{k}\sigma}(1-f^j_{\tilde{k}+\tilde{q},\sigma})\times\delta(\hbar\omega-[\Delta E(\tilde{k},\tilde{q})]_{ij}) \quad , \tag{2}$$

where Ω is the volume. The sum $\sum_{ij}$ ranges over all pairs of valleys i and j (including $i=j$) where the transitions take a carrier from valley i to valley j. The occupation probability of a state in the ith valley with momentum $\tilde{k}$ and spin σ is $f^i_{\tilde{k}\sigma}$ and $[\Delta E(\tilde{k},\tilde{q})]_{ij}$ is the difference in energy between electronic states $(\tilde{k}+\tilde{q},\sigma)_j$ and $(\tilde{k}\sigma)_i$. With $E\equiv 0$ at the appropriate (electron or hole) quasi-Fermi level and $\tilde{k}\equiv 0$ at zone center, the energy of a carrier in state $(\tilde{k}\sigma)_i$ is

$$E^i_{\tilde{k}}=E_i+\frac{\hbar^2(\tilde{k}-\tilde{Q}_{0i})^2}{2m_i^*} \quad ,$$

where E_i and $\tilde{Q}_{0i}$ are the energy and wave vector of the ith valley minimum. Each valley i has been approximated by spherical constant energy surfaces characterized by effective mass m_i^*. At high enough temperatures, the occupation probabilities are essentially Boltzmann, so that $f^i_{\tilde{k}\sigma}\approx e^{-\beta E^i_{\tilde{k}}}$ and $f(1-f)\approx f$. Equation (2) can then be written

$$\epsilon_2(\tilde{q},\omega)=\frac{8\pi^2e^2}{\Omega q^2}\sum_{ij}\sum_{\tilde{k}}e^{-\beta E^i_{\tilde{k}}}\delta(\hbar\omega-(E^j_{\tilde{k}+\tilde{q}}-E^i_{\tilde{k}}))$$

$$=\frac{8\pi^2e^2}{\Omega q^2}\sum_{ij}e^{-\beta E_i}\sum_{\tilde{k}}\exp[-\beta\hbar^2(\tilde{k}-\tilde{Q}_{0i})^2/2m_i^*]\times\delta\left\{\hbar\omega-\left[(E_j-E_i)+\left[\frac{\hbar^2}{2m_j^*}(\tilde{k}+\tilde{q}-\tilde{Q}_{0j})^2-\frac{\hbar^2}{2m_i^*}(\tilde{k}-\tilde{Q}_{0i})^2\right]\right]\right\} \quad . \tag{3}$$

Equation (3) is a generalization of the expression derived previously[1] for the case $E_i=E_j$ and $m_i^*=m_j^*$. With the substitution $\tilde{k}'\equiv\tilde{k}-\tilde{Q}_{0i}$ and with $\tilde{Q}_{ij}\equiv[\tilde{q}+(\tilde{Q}_{0i}-\tilde{Q}_{0j})]\equiv(\tilde{q}-\tilde{Q}_{0ij})$ and Θ_{ij} the angle between $\tilde{k}'$ and $\tilde{Q}_{ij}$, Eq. (3) can be written

$$\epsilon_2(\tilde{q},\omega)=\frac{2e^2}{q^2}\sum_{ij}e^{-\beta E_i}\int k'^2\,dk'\,d\cos\Theta_{ij}\exp(-\beta\hbar^2k'^2/2m_i^*)\times\delta\left\{\hbar\omega-\left[(E_j-E_i)+\left[\frac{\hbar^2}{2m_j^*}(k'^2+Q_{ij}^2+2k'Q_{ij}\cos\Theta_{ij})-\frac{\hbar^2k'^2}{2m_i^*}\right]\right]\right\} \quad . \tag{4}$$

Integrated over the δ function, Eq. (4) becomes

$$\epsilon_2(\tilde{q},\omega)=\frac{2e^2}{q^2}\sum_{ij}e^{-\beta E_i}\int_{k'^2_{\min}}^{k'^2_{\max}}\frac{\exp(-\beta\hbar^2k'^2/2m_i^*)\,d(k'^2)}{(2\hbar^2/m_j^*)Q_{ij}} \quad , \tag{5a}$$

where

$$\frac{\hbar^2k'^2_{\min/\max}}{2m_i^*}=4E_{Q_{ij}}\frac{m_j^*}{m_i^*}\frac{1-2M_{ij}E_{ij}\mp(1-4M_{ij}E_{ij})^{1/2}}{2M_{ij}^2} \quad , \tag{5b}$$

with $M_{ij}=(m_j^*/m_i^*-1)$, $E_{ij}=[\hbar\omega-(E_j-E_i)-E_{Q_{ij}}]/4E_{Q_{ij}}$, and $E_{Q_{ij}}=\hbar^2Q_{ij}^2/2m_j^*$. Equation (5b) requires $4M_{ij}E_{ij}\leq 1$, i.e., $(1-m_i^*/m_j^*)[\hbar\omega-(E_j-E_i)]\leq E_{Q_{ij}}$. If this condition is not met, there is no phonon which can connect the two valleys. With the definitions (5b), the final result is

$$\epsilon_2(\tilde{q},\omega)=\frac{4e^2}{q^2}\sum_{ij}e^{-\beta E_i}\frac{m_i^*m_j^*}{\beta\hbar^4Q_{ij}}\times\exp\left[-4\frac{m_j^*}{m_i^*}\beta E_{Q_{ij}}\frac{(1-2M_{ij}E_{ij})}{2M_{ij}^2}\right]\sinh\left[4\frac{m_j^*}{m_i^*}\beta E_{Q_{ij}}\frac{(1-4M_{ij}E_{ij})^{1/2}}{2M_{ij}^2}\right] \quad . \tag{6}$$

This solution can now be examined for those transitions—intravalley and both equivalent and inequivalent intervalley— relevant to hot-carrier relaxation. For intravalley transitions, that is, when $i=j$, one has $M_{ij}=0$ so that Eq. (6) reduces to the familiar result

$$\epsilon_2(\tilde{q}\omega)=\frac{e^2}{q^2\hbar^3\beta^{3/2}}(8\pi)^{1/2}\sum_i e^{-\beta E_i}m_i^{*3/2}\frac{\exp[-\beta(\hbar\omega-E_q)^2/4E_q]}{(4\pi E_q/\beta)^{1/2}} \quad . \tag{7}$$

Here ϵ_2 has a peak at $\hbar\omega = E_q = \hbar^2 q^2/2m_i^*$, of width $\hbar\Gamma_{ii} = \sqrt{2E_q/\beta}$. For equivalent valleys i and j ($m_i^* = m_j^*$, $E_i = E_j$), ϵ_2 takes the same form as in Eq. (7), except that now the sum is taken over all *pairs* of valleys ij. Again, $M_{ij} = 0$, so that

$$k_{\min} = \left| \frac{m_i^*}{\hbar^2 Q_{ij}} (\hbar\omega - E_{Q_{ij}}) \right|$$

and $k_{\max} \to \infty$. ϵ_2 peaks at $\hbar\omega = E_{Q_{ij}} = \hbar^2(\tilde{q} - \tilde{Q}_{0ij})^2/2m_j^*$. Here, $\hbar\Gamma_{ij} = \sqrt{2E_{Q_{ij}}/\beta}$.

The situation for inequivalent valleys ($m_i^* \neq m_j^*$, $E_i \neq E_j$) is more complicated, as seen from Eq. (6). Figure 1 shows the dependence of $\epsilon_2(\tilde{q}, \omega)$ on $\hbar\omega$ (strictly, on $x = 2M_{ij}E_{ij} = (m_j^*/m_i^* - 1)[\hbar\omega - (E_j - E_i) - E_{Q_{ij}}]/2E_{Q_{ij}}$), with C as a parameter; C is defined by

$$C \equiv 2\beta E_{Q_{ij}} \frac{m_j^*/m_i^*}{(m_j^*/m_i^* - 1)^2} .$$

C and, consequently, ϵ_2, depend strongly on the angle between $\tilde{q}$ and $\tilde{Q}_{0ij}$. [It should be noted that although the peaks broaden as C decreases due to the $E_{Q_{ij}}$ in the denominator of x, the actual peak widths $\Delta(\hbar\omega)$ are not functions of C.]

For $C \lesssim 0.5$, $\epsilon_2(\tilde{q}, \omega)$ has an asymmetric maximum of approximate width $\hbar\Gamma_{ij} = |1 - m_i^*/m_j^*|/\beta$ at

$$\hbar\omega = (E_j - E_i) + \frac{m_i^*/m_j^* - 1}{2\beta} . \tag{8}$$

This result can be understood by considering the simple case $Q_{ij} = 0$ ($C \equiv 0$), for which the change in carrier momentum during the transition is exactly equal to the wave-vector separation between valley minima.

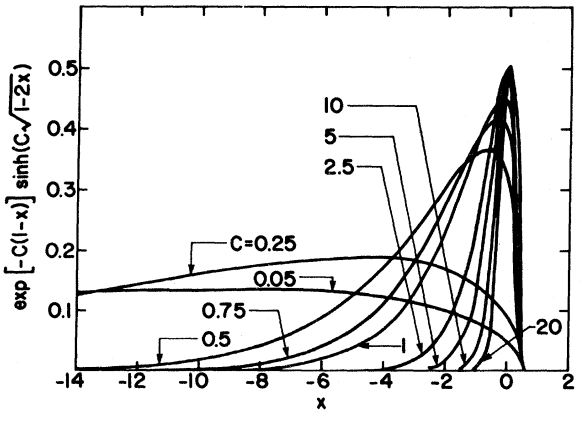

FIG. 1. Dependence of $\epsilon_2(\tilde{q}, \omega)$ on $\hbar\omega$, with C as a parameter. The function plotted is proportional to $\epsilon_2(\tilde{q}, \omega)$ and the horizontal axis x is $x \equiv (m_j^*/m_i^* - 1)[\hbar\omega - (E_j - E_i) - E_{Q_{ij}}]/2E_{Q_{ij}}$. The parameter $C \equiv 2\beta E_{Q_{ij}}(m_j^*/m_i^*)/(m_j^*/m_i^* - 1)^2$.

This transition is illustrated in Fig. 2 for initial carrier energy E^i. The momentum of the carrier with respect to these minima is not changed by the transition:

$$2m_i^*(E^i - E_i)/\hbar^2 = 2m_j^*(E^j - E_j)/\hbar^2 ,$$

so that the net change in energy is

$$\hbar\omega = E^j - E^i = (E_j - E_i) + (E^i - E_i)(m_i^*/m_j^* - 1) .$$

$(E^i - E_i)$ is just the initial energy of the carrier relative to the band edge. For a thermalized distribution, the energy probability has a maximum at $1/2\beta$ and Eq. (8) is obtained. When $C \gtrsim 1.5$, ϵ_2 has a peak of width $[(2E_{Q_{ij}}/\beta)(m_i^*/m_j^*)]^{1/2}$ at $\hbar\omega = (E_j - E_i) + E_{Q_{ij}}$.

The above described structure in $\epsilon_2(\tilde{q}, \omega)$ is summarized in Table I. When the peaks in ϵ_2 are replaced by normalized Lorentzians having appropriate peak locations and widths, the Kramers-Kronig relations can be used to construct ϵ_1 and the excitation spectrum. All of the transitions can be represented by expressions of the same form, with the exception that the factor $m_i^{*3/2}$ appearing in Eq. (7) is replaced by $m_i^{*3/2}(m_j^*/m_i^*)^{1/2}$. When i is taken to refer to the set of g_i equivalent valleys i, the imaginary part of the dielectric function becomes

$$\epsilon_2(\tilde{q}, \omega) = \epsilon_0 \sum_{(ij)} (\hbar\omega_{pi})^2 \times f_{ij} \frac{(\hbar\Gamma_{ij})(\hbar\omega)}{[(\hbar\Omega_{ij})^2 - (\hbar\omega)^2]^2 + (\hbar\Gamma_{ij})^2(\hbar\omega)^2} , \tag{9}$$

where $\hbar\Omega_{ij}$ is the peak location and $\omega_{pi} \equiv (4\pi N_i e^2/\epsilon_0 m_i^*)^{1/2}$, with N_i the number of carriers in valleys i and ϵ_0 the bulk dielectric function. ϵ_0 represents the contribution from interband (valence-to-conduction) transitions, so that $\epsilon_0(\tilde{q}, \omega) \approx \epsilon_0(\tilde{q}, \omega \approx 0)$ and $\mathrm{Im}\epsilon_0$

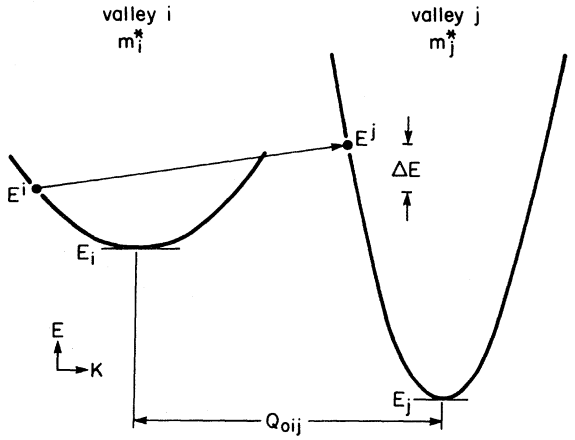

FIG. 2. Transition from valley i to valley j for the case $Q_{ij} = 0$ ($C \equiv 0$). $\Delta E = (E_j - E_i) + (E^i - E_i)(m_i^*/m_j^* - 1)$.

TABLE I. Contributions to ϵ_2 from different transition types.

Transition	Peak position $\hbar\Omega_{ij}$	Peak width $\hbar\Gamma_{ij}$
Intravalley	$\frac{\hbar^2 q^2}{2m_i^*}$	$\left(\frac{2E_q}{\beta}\right)^{1/2}$
Intervalley (Equivalent valleys)	$\frac{\hbar^2 Q_{ij}^2}{2m_i^*}$	$\left(\frac{2E_{Q_{ij}}}{\beta}\right)^{1/2}$
Intervalley (Inequivalent valleys)		
$C \lesssim 0.5$	$(E_j - E_i) + \frac{1}{2\beta}\left(\frac{m_i^*}{m_j^*} - 1\right)$	$\frac{1}{\beta}\left\|1 - \frac{m_i^*}{m_j^*}\right\|$
$C \gtrsim 1.5$	$(E_j - E_i) + E_{Q_{ij}}$	$\left(\frac{2E_{Q_{ij}}}{\beta}\frac{m_i^*}{m_j^*}\right)^{1/2}$

is negligible at those phonon frequencies with which we are concerned. f_{ij} is the effective oscillator strength for the transition,

$$f_{ij} = Z_{ij}\left(\frac{m_j^*}{m_i^*}\right)^{1/2}\frac{\hbar\Omega_{ij}}{E_q} .$$

Z_{ij} is the number of intravalley or intervalley transitions with resonances at $\hbar\omega = \hbar\Omega_{ij}$. In other words, the sum (ij) is taken over distinguishable ij pairs, so that $\Omega_{ij} \neq \Omega_{kl}$ for all $ij \neq kl$. For intravalley transitions, e.g., f_{ij} reduces to 1.

Because the cross terms for different resonances Ω_{ij} are negligibly small, the excitation spectrum becomes

$$\mathrm{Im}\frac{1}{\epsilon(\tilde{q},\omega)} = \frac{1}{\epsilon_0}\left[\sum_{(ij)} Z_{ij}(\hbar\omega_{pi})^2\left(\frac{m_j^*}{m_i^*}\right)^{1/2}\frac{\hbar\Omega_{ij}}{E_q}\frac{(\hbar\Gamma_{ij})(\hbar\omega)}{[(\hbar\Omega_{ij})^2-(\hbar\omega)^2]^2+(\hbar\Gamma_{ij})^2(\hbar\omega)^2}\right]$$

$$\times\left[\sum_{(ij)}\frac{[(\hbar\Omega_{ij})^2-(\hbar\omega)^2+Z_{ij}(\hbar\omega_{pi})^2(m_j^*/m_i^*)^{1/2}\hbar\Omega_{ij}/E_q]^2+(\hbar\Gamma_{ij})^2(\hbar\omega)^2}{[(\hbar\Omega_{ij})^2-(\hbar\omega)^2]^2+(\hbar\Gamma_{ij})^2(\hbar\omega)^2}\right]^{-1} . \quad (10)$$

For each pair of valleys, there is a contribution to the excitation spectrum when $\Omega_{ij}(\tilde{q}) \approx \omega$. This condition selects those values of $\tilde{q}$, $\tilde{q}_{0ij}$, which dominate transitions from valley i to valley j. Equation (10) can then be approximated by

$$\mathrm{Im}\frac{1}{\epsilon(\tilde{q},\omega)} \approx \frac{1}{\epsilon_0}\sum_{(ij)}\frac{Z_{ij}(\hbar\omega_{pi})^2(m_j^*/m_i^*)^{1/2}(\hbar\Gamma_{ij})(\hbar\omega)^2/E_q}{Z_{ij}^2(\hbar\omega_{pi})^4(m_j^*/m_i^*)(\hbar\omega/E_q)+(\hbar\Gamma_{ij})^2(\hbar\omega)^2}\delta_{\tilde{q},\tilde{q}_{0ij}} , \quad (11)$$

where $\Omega_{ij}(\tilde{q}_{0ij}) \approx \omega$.

The values found for $\tilde{q}_{0ij}$ are locations of wave-vector resonances of $q^2\epsilon_2(\tilde{q},\omega)$. As will be shown shortly the phonon emission rate $R_{\tilde{q},\omega}$ is proportional to $q^2\epsilon_2|V|^2$. For nonpolar intravalley transitions, $q_{0ij} = q_{0ii} = (2m_i^*\omega/\hbar)^{1/2}$. For transitions between valleys, the position of the resonance depends on the angle α between $\tilde{q}$ and $\tilde{Q}_{0ij}$. In this case, with

$$q_{\Delta E_{ij}}^2 \equiv 2m_j^*(E_i - E_j)/\hbar^2,$$

$$q_{0ij} = Q_{0ij}\left\{\cos\alpha \pm \left[(\cos^2\alpha - 1) + \left(\frac{q_{\Delta E_{ij}}^2 + 2m_j^*\omega/\hbar}{Q_{0ij}^2}\right)\right]^{1/2}\right\} .$$

When the valleys are equivalent, $q_{\Delta E_{ij}} = 0$. Here, be-

cause the phonon energy is much less than $E_{Q_{0ij}}=\hbar^2Q_{0ij}^2/2m_j^*$, the phonon wave vector is nearly equal to the wave vector connecting the two valleys. That is, $\tilde{q}\approx\tilde{Q}_{0ij}$. When $E_i\neq E_j$ and $\tilde{q}$ is parallel to Q_{0ij} ($\cos\alpha=1$), $q_{0ij}\approx|Q_{0ij}\pm q_{\Delta E_{ij}}|$. When the vectors are perpendicular ($\cos\alpha=0$) and $q_{\Delta E_{ij}}>Q_{0ij}$, $q_{0ij}\approx(q_{\Delta E_{ij}}^2-Q_{0ij}^2)^{1/2}$. When $q_{\Delta E_{ij}}<Q_{0ij}$, the most likely transition occurs at q near zero, but with probability down by a factor $\exp[-\beta(Q_{0ij}^2-q_{\Delta E_{ij}}^2)/(m_j^*/m_i^*-1)]$. In each of the above cases, the values of $\tilde{q}_{0ij}$ can be simply understood by recognizing that the Boltzmann factor favors those transitions originating from as deep within a band as possible.

The rate for emission of phonons (wave vector $\tilde{q}$, frequency ω) is given within the random-phase approximation by the golden rule[26] to be

$$R_{\tilde{q},\omega}=\frac{2\pi}{\hbar}\sum_{ij}\sum_{\tilde{k}\sigma}\left|\frac{V_{\tilde{k}+\tilde{q},\tilde{k}}^{ij}}{\epsilon}\right|^2 f_{\tilde{k}+\tilde{q},\sigma}^{i}(1-f_{\tilde{k}\sigma}^{j})\delta(\hbar\omega-(E_{\tilde{k}+\tilde{q}}^{i}-E_{\tilde{k}}^{j})) \quad , \tag{12}$$

where $V_{\tilde{k}+\tilde{q},\tilde{k}}^{ij}$ is the unscreened matrix element for the transition of an electron from state $(\tilde{k}+\tilde{q})_i$ to state $(\tilde{k})_j$ via phonon emission. Because the carrier temperature greatly exceeds the lattice temperature, phonon absorption makes negligible contribution to the net energy relaxation rate of the carriers. (See, however, Sec. IV.) V depends not only on the wave vector of the phonon emitted, but also on the particular type of coupling between valleys i and j. With the usual assumption that V does not depend strongly on electronic state k, and using Eq. (11), Eq. (12) can be written in the form

$$R_{\tilde{q},\omega}=\frac{\Omega e^{-\beta\hbar\omega}}{\pi\hbar e^3\epsilon_0^2}\sum_{(ij)}|V_q^{ij}|^2Z_{ij}\frac{(\hbar\omega_{pi})^2}{(\hbar\Gamma_{ij})}\frac{(m_j^*)^{3/2}}{(m_i^*)^{1/2}}\delta_{\tilde{q},\tilde{q}_{0ij}}\Bigg/\left[1+\frac{Z_{ij}^2(\hbar\omega_{pi})^4}{(\hbar\Gamma_{ij})^2E_q^2}\frac{m_j^*}{m_i^*}\right] \quad , \tag{13}$$

where the screening effect of the excited carriers is shown explicitly. As expected, only carriers within valley i contribute to screening of the i to j transitions at $(\tilde{q},\omega)$. This is a consequence of the fact that these transitions are screened only by those carriers which can respond at $(\tilde{q},\omega)$, in other words, those carriers within valleys i. Each $\tilde{q}_{0ij}$ corresponds to a shell of preferred $\tilde{q}$'s. For example, for intravalley transitions, R peaks at each $\tilde{q}$ such that $|\tilde{q}|=q_{0ii}$. This criterion leads to $4\pi q_{0ii}^3(\Delta q_{0ii})(2\pi)^3/(a^3/4)$ distinct $\tilde{q}$ values, where the peak width $\hbar\Gamma_{ii}$ determines Δq_{0ii}. Because this density-of-states factor is the same for each transition (as a result of the correspondence between transitions found in Ref. 1) it need not be included explicitly in determining relative emission rates.

The carrier density dependence of the various emission rates can be seen more clearly by recognizing that $(\hbar\omega_{pi})^2\sim N_i$, where N_i is the density of carriers in valleys i. The critical value of N_i for the onset of screening is

$$(N_{ic})_{ij}=\frac{\epsilon_0(\hbar\Gamma_{ij})q_{0ij}^2}{8\pi e^2Z_{ij}}\left(\frac{m_i^*}{m_j^*}\right)^{3/2} \quad . \tag{14}$$

As expected, large wave-vector transitions are more difficult to screen. Also, the critical density increases weakly with temperature [$\Gamma\sim(kT)^{1/2}$].

III. Si AND GaAs COMPARED

Actual phonon emission rates depend strongly on the nature of the carrier–optical-phonon couplings V_q^{ij}. Energy relaxation via acoustic-phonon emission is less efficient and dominates only when the carriers have already relaxed to within an optical-phonon energy of the band edge. In the case of nonpolar materials, matrix elements for optical-phonon emission do not in general depend on the phonon wave vector q, whereas for polar interactions,[27,28] $V\sim 1/q$. With knowledge of the particular types of coupling which are operative for specific intravalley and intervalley transitions, Eq. (13) can be used to calculate the rates accurately. However, even without a detailed determination of precise coupling strengths, it is possible to compare the effects of high densities of excited carriers on each kind of transition in a given material.

With the expressions for the widths Γ derived in Sec. II, Eq. (14) can be used to determine the critical density of carriers in valley i for each type of transition.[29] For intravalley transitions,

$$(N_{ic})_{ii}=\frac{\epsilon_0\hbar q_{0ii}^3}{8\pi e^2}\left(\frac{1}{\beta m_i^*}\right)^{1/2} \quad , \tag{15}$$

where $q_{0ii}=(2m_i^*\omega/\hbar)^{1/2}$ for nonpolar Si and as will be shown, $q_{0ii}=(\beta m_i^*/3)^{1/2}\omega$ for polar GaAs. For equivalent intervalley transitions,

$$(N_{ic})_{ij}=\frac{\epsilon_0Q_{0ij}^2}{8\pi e^2Z_{ij}}\left(\frac{2\hbar\omega}{\beta}\right)^{1/2} \quad . \tag{16}$$

Finally, for transitions between inequivalent valleys,

$$(N_{ic})_{ij}=\frac{\epsilon_0Q_{0ij}^2}{8\pi e^2Z_{ij}}\left(\frac{m_i^*}{m_j^*}\right)^2\left(\frac{2(E_i-E_j)}{\beta}\right)^{1/2} \quad . \tag{17}$$

β in these equations refers to the carrier temperature

established by the carrier thermalization process. The relative importance of electron-hole pair creation and free-carrier absorption is not important if carrier thermalization is more rapid than phonon emission. As discussed above, for high carrier densities in Si, the recombination is predominantly Auger so that energy is retained by and rearranged within the system of carriers. On the other hand, in GaAs much of the energy is radiated away from the carriers during recombination. If recombination is slow compared with times of interest, the number and energy density of the carriers are simply related to the intensity and wavelength of the laser pulse. In fact, the greater the extent to which the recombination time exceeds the laser pulse duration, the greater the quasi-Fermi level splitting and the lower the carrier temperature (for given total carrier energy). Provided the total carrier number and energy densities are known, the carrier temperature (and quasi-Fermi levels) can be calculated.

As found previously,[1] the relevant phonon wave vectors for emission in Si are $q \approx 6.6\times10^{6}$, 4.6×10^{7}, and 1.2×10^{8} cm^{-1} for intravalley, intervalley on-axis (f), and intervalley off-axis (g) transitions, respectively. Within the hole band, the important values of q are 4.6×10^{6} and 8.1×10^{6} cm^{-1}. For GaAs, the polar coupling $V\sim 1/q$ shifts the intravalley peak positions to smaller wave vector. For these transitions, $q_{0ii}\rightarrow\omega(\beta m_i^*/3)^{1/2}$. The wave vectors which dominate intravalley relaxation are then $q\approx 6.0\times10^{5}$ cm^{-1} for the conduction-band minimum at zone center ($m^*=0.067m$, $g=1$)[30] and 1.1×10^{6} and 1.5×10^{6} cm^{-1} for the heavy-mass valleys at the L ($\Delta E=0.29$ eV, $g=4$, $g^{2/3}m^*=0.55m$)[30] and X ($\Delta E=0.48$ eV, $g=3$, $g^{2/3}m^*=0.85m$)[30] points, respectively. For holes, the relevant values of q are 8.0×10^{5} and 1.6×10^{6} cm^{-1}. At large wave vectors appropriate to intervalley transitions, the polar interaction is less effective and relaxation proceeds through a deformation-type coupling similar to that in nonpolar semiconductors such as Si and Ge. Because $q_{\Delta E}\ll Q_0$, transitions from these heavy-mass valleys to the minimum at the center of the zone occur at $q\approx 9.6\times10^{7}$ cm^{-1} and 1.1×10^{8} cm^{-1}. Those among equivalent higher-energy valleys are peaked at $q\approx 1.1\times10^{8}$ cm^{-1}.

The critical densities for Si and GaAs calculated from Eqs. (15)–(17) are listed in Table II, with the particular choice $\beta=10$ eV^{-1}. (Efficient carrier relaxation via optical-phonon emission requires the initial carrier temperature to be at least comparable to the optical-phonon energy.) The table shows both the critical density of carriers N_{ic} *in the set of valleys* i required to screen the $i\rightarrow j$ transitions and the *total* carrier density N_c corresponding to N_{ic}. The values of N_{ic} do not depend strongly on β in this temperature regime, since $\beta^{1/2}$ varies only by a factor of approximately 2–3 as the temperature ranges from that appropriate to pulsed laser annealing conditions to that of the pulse-probe experiments mentioned earlier. (Although the total carrier energy density in the former situation greatly exceeds that in the latter, the

TABLE II. Critical carrier densities within valley i (N_{ic}) and critical total carrier densities (N_c) for $i\rightarrow j$ transitions in Si and GaAs. The calculated carrier densities for screening of the X–L, L–Γ, and X–Γ transitions exceed possible values.

	Si			GaAs	
	N_{ic} (cm^{-3})	N_c (cm^{-3})		N_{ic} (cm^{-3})	N_c (cm^{-3})
Intravalley transitions			Intravalley transitions		
Electrons			Electrons		
	1.4×10^{19}	1.4×10^{19}	Γ	2.2×10^{16}	6.0×10^{16}
			L	7.4×10^{16}	1.5×10^{17}
			X	1.4×10^{17}	1.0×10^{18}
Holes			Holes		
lh	6.9×10^{18}	4.5×10^{19}	*lh*	3.9×10^{16}	3.7×10^{17}
hh	2.2×10^{19}	2.6×10^{19}	*hh*	1.5×10^{17}	1.7×10^{17}
Intervalley transitions			Intervalley transitions		
on-axis (f)	6.9×10^{20}	6.9×10^{20}	L–L	1.0×10^{21}	1.8×10^{21}
off-axis (g)	1.2×10^{21}	1.2×10^{21}	X–X	1.5×10^{21}	3.7×10^{21}
			X–L	4.7×10^{21}	. . .
			L–Γ	9.4×10^{22}	. . .
			X–Γ	4.0×10^{23}	. . .

different quasi-Fermi-level splittings lead to carrier temperatures which are relatively similar for the two cases.) In support of this, it should be noted that the onset of the decrease in the cooling rate of photoexcited carriers in GaAs was measured to be independent of carrier temperature.[17] However, the energy relaxation rate was found to fall with decreasing excess carrier energy[16] and with time after excitation.[11] In both cases, the concomitant decrease in carrier temperature would be expected to reduce the relaxation rate as a result of the factor $N_i(\beta)\exp(-\beta\hbar\omega)$ in Eq. (13).

For Si, with just one type of relevant conduction-band valley, $N = N_i$. Thus, from Eq. (13), the i to j transition rate has the dependence

$$R^{ij}_{\vec{q},\omega} \sim N \Big/ \left[1 + \left(\frac{N}{N_{cij}}\right)^2\right] . \tag{18}$$

N_{cij} is the value of the *total* carrier density at which screening effects appear and is given in this case by Eq. (14). The emission frequency, which is $\nu^{ij}_{\vec{q},\omega} = R^{ij}_{\vec{q},\omega}/N$, is then

$$\nu^{ij}_{\vec{q},\omega} \sim 1 \Big/ \left[1 + \left(\frac{N}{N_{cij}}\right)^2\right] . \tag{19}$$

Strictly speaking, the N dependence of the screening factor in Eq. (19) is not precisely $[1+(N/\text{const})^2]^{-1}$ because the "const" N_c itself depends on N through β. However, $\beta^{-1/2}$ is roughly proportional to $(\ln N)^{-1/2}$ so that N_c varies only weakly with N. For small N, ν is independent of N. When N grows very large, $\nu \sim N^{-2}$. In this case, screening by the excited carriers more than compensates for the increase in carrier density so that even the scattering rate Eq. (18) decreases with increasing N. The change in character of the N dependence occurs at the critical value N_{cij}. For intravalley transitions within the valence bands of Si, the emission frequency is given by Eq. (19) with the critical total carrier density

$$N_{cii} = \frac{\epsilon_0(\hbar\Gamma_{ii})q^2_{0ii}}{8\pi e^2}\left[1 + \left(\frac{m^*_{kh}}{m^*_{ih}}\right)^{3/2}\right] , \tag{20}$$

where $i = l$ and $k = h$ ($i = h$ and $k = l$) for light- (heavy-) hole transitions. Transitions between valence bands can be treated in the same manner as intervalley electronic transitions, but will not be explicitly discussed here. However, because both hole bands lie at the center of the Brillouin zone, the critical density for transitions between them will be less than that for intravalley transitions within the heavy-hole band.

By applying the analytic methods of Joyce[31] and Joyce and Dixon[32] to GaAs, the individual valley densities N_{ic} in Eqs. (15)–(17) can be related to critical values of *total* photoexcited carrier densities. Because of the large density of states in the L and X valleys, a significant fraction of the excited carriers lies in these valleys. (To illustrate this fact: the total density given in Table II for screening within the L valleys is less than that for the Γ valley, even though $N_{Lc_{LL}} > N_{\Gamma c_{\Gamma\Gamma}}$.) From Eq. (13), the phonon emission frequency is

$$\nu^{ij}_{\vec{q},\omega} \sim \left(\frac{N_i}{N}\right) \Big/ \left[1 + \left(\frac{N_i}{(N_{ic})_{ij}}\right)^2\right] . \tag{21}$$

For N in the range $N_{c\,(\text{intravalley})} < N < N_{c\,(\text{intervalley})}$, the overall emission frequency is sensitive to the strength of the intervalley matrix element as compared with the polar coupling within a valley. However, if the coupling strengths are comparable, relaxation by unscreened intervalley transitions will occur rapidly until large wave-vector phonons can no longer dominate the relaxation, i.e., until a large fraction of the carriers do not have sufficient energy to make it to the higher valleys. If the intervalley coupling is much weaker, the overall emission rate will be significantly reduced. Because the ratios N_i/N are not functions of the energy-band gap, the dependence of this energy on carrier temperature[33] and density[34] can be neglected.

At these high concentrations, the carriers are in communication through extremely rapid Coulomb collisions. Carrier energy will consequently escape to the lattice via the fastest available channel. As a result, electrons and holes lose energy at essentially the same per carrier rate,

$$\frac{dE}{dt} = \sum_{(ij)} \nu^{ij}_{\vec{q},\omega}\hbar\omega . \tag{22}$$

The emission frequencies relevant to Si [Eq. (19)] and GaAs [Eq. (21)] are plotted as functions of carrier density in Figs. 3(a) and 3(b), respectively. In each case, large wave-vector intervalley phonons remain unscreened until very high carrier density. In fact, the calculated critical densities for transitions between the higher-energy valleys in GaAs will never be achieved. The contrast between Si and GaAs is readily apparent from Fig. 4, where the carrier dependences of the total emission rates for the two semiconductors are plotted. First, essentially *all* of the excited electrons in Si can emit large wave-vector intervalley phonons. In GaAs, only those carriers with at least 0.28 eV of excess energy (the Γ–L separation)[30] can make transitions between valleys. However, as explained above, the large effective masses in the L and X valleys do lead to reasonably large values of N_L/N and N_X/N. More important is the fact that in Si the mechanism for intravalley carrier-phonon scattering is the same as for equivalent and inequivalent intervalley transitions, with similar deformation potentials. The interaction matrix element V has therefore been taken to be the same for all five

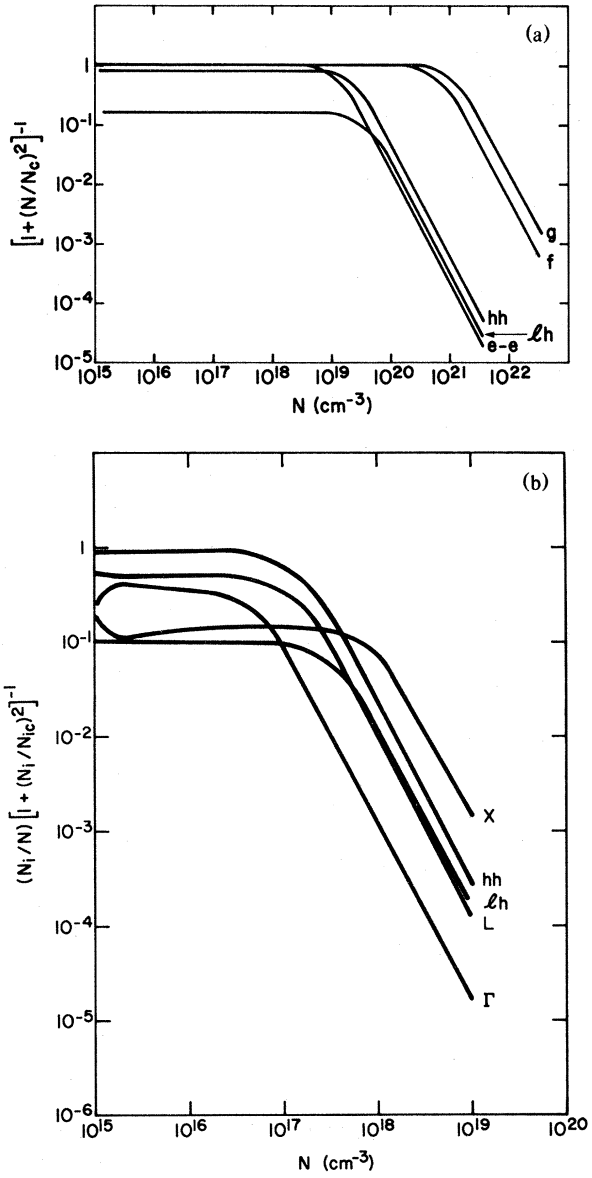

FIG. 3. Dependence on total carrier density of phonon emission frequencies for the relevant transitions in (a) Si and (b) GaAs.

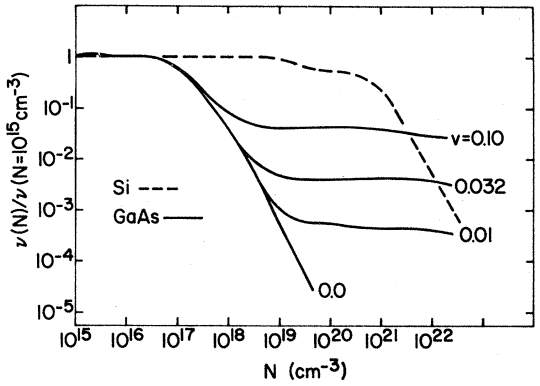

FIG. 4. Dependence of total phonon emission frequencies on total carrier density for Si and GaAs, normalized to their values at $N = 10^{15}$ cm^{-3}. For GaAs, the frequencies are plotted for several values of the parameter $\nu \equiv V_{\text{inter}}/V_{\text{intra}}(q = 6\times 10^5$ cm$^{-1})$.

of the transitions in Si. The resultant total emission frequency plotted in Fig. 4 remains large until very large N. On the other hand, the polar Fröhlich interaction which dominates small-q intravalley transitions in GaAs is much less important for transitions between valleys, which proceed instead via a deformation coupling similar to that for intervalley transitions in Si. Using deformation potentials cited by Fawcett *et al.*[35] the intervalley transition matrix elements are found to be reduced by factors 0.1–0.01 from those appropriate to the intravalley couplings.

Figure 4 shows the total emission frequency in GaAs (normalized to its value at $N = 10^{15}$ cm^{-3}), for several values of $\nu \equiv V_{\text{inter}}/V_{\text{intra}}(q = 6\times 10^5$ cm$^{-1})$. Note that although the intervalley transitions in GaAs are just as difficult to screen as those in Si, the screening of the small-q intravalley transitions in GaAs should be observed when the density exceeds the critical values for these transitions. Consequently, a reduction in the energy relaxation rate in GaAs should occur at attainable carrier densities; the high densities required for an appreciable reduction in Si suggest that screening effects in this material are unlikely to appear.

IV. DISCUSSION

As mentioned earlier, Leheny *et al.*[17] have observed a decrease in the initial hot-carrier cooling rate in GaAs at photoexcited carrier densities greater than $\sim 10^{17}$ cm^{-3}. Below that density the cooling rate was determined to be independent of N. Although at densities exceeding $\sim 10^{18}$ cm^{-3} the carrier distribution remains nonthermalized for times as long as 10 ps following excitation,[17] the rate of cooling appears to decrease by roughly a factor of 5 when a density of 10^{18} cm^{-3} is attained. Indeed, the above calculations indicate a density-independent energy relaxation rate at moderate densities. They predict that the onset of screening should occur at $N \approx 6\times 10^{16}$ cm^{-3}, at which density screening of phonon emission by electrons in the central valley becomes effective. With the assumption that the hole-phonon coupling strength is comparable to that between electrons and phonons, the energy relaxation rate should be reduced by roughly one-quarter at this density, and by a factor of ~ 7–10 by $N \sim 5\times 10^{17}$ cm^{-3}. At higher

densities, the relaxation rate decreases rapidly with N. The calculated behavior is therefore qualitatively similar to that observed; the quantitative difference between calculated and measured critical densities is not yet understood, but given the crudeness of the calculation, is probably not significant. (The reason the carriers fail to thermalize as rapidly at very high as at moderate densities has not been explained. As discussed at length above, the calculations in this paper assume thermalization has occurred.) To the author's knowledge, consistent with expectations, no reduction in the carrier cooling rate in indirect-gap semiconductors such as Si and Ge has been experimentally observed.

The methods developed in the preceding sections can of course be applied to other direct- and indirect-gap semiconductors. For the band structure of Ge, it appears likely that large-q intervalley phonon emission remains unscreened even at high carrier densities. Photoexcited carrier temperatures greatly in excess of lattice temperatures have been measured in CdS (Refs. 36 and 37) and CdSe (Ref. 38) although time-resolved spectroscopic measurements capable of monitoring the hot-carrier cooling rate have not yet been performed. The above calculations suggest that screening of the phonon emission should be attainable in these systems. In Sec. III the critical carrier density N_{ic} for the onset of screening in direct-gap, polar semiconductors was shown to vary as $\epsilon_0 m_i^* \omega^3$. This result can be used to predict *trends* among polar semiconductors (e.g., GaAs, CdS, CdSe, InAs, InP, InSb, etc.) in the effectiveness of screening.

Nonequilibrium phonon distributions generated during hot-carrier relaxation provide an interesting related topic for study.[39–42] When the phonon equilibrium time exceeds the emission time, interesting phonon bottleneck effects can occur. Because phonon emission is strongly peaked at wave vectors specific to the particular band structure, the phonon population will build up preferentially at certain locations in the Brillouin zone (local "hot spots" in q space). If the population of emitted phonons grows large enough, these same phonons will be reabsorbed by the carriers.[43] This process consequently adds to the effect of screening to decrease the net rate of carrier cooling. von der Linde[42] has found that the rise time for the population of near-zone-center phonons ($q < 8 \times 10^5$ cm^{-1}) in GaAs with $N \sim 10^{17}$–10^{18} cm^{-3} is less than ~4 ps, although the density dependence of this time has not yet been investigated.

The calculations in this paper describe the relaxation of hot carriers comprising thermalized distributions (characterized by a carrier temperature and electron and hole quasi-Fermi levels). As such, the phonon emission rates derived refer to relaxation of the distribution as a whole. As discussed above, the spectrum of emitted phonons is strongly peaked at those wave vectors corresponding to transitions originating from states near the valley minima, i.e., those states most likely to be occupied. A complementary approach to the problem of hot-carrier relaxation is the investigation of phonon emission by one or more hot carriers in nonthermalized distributions, e.g., distributions peaked at the excitation energy. In this case, the $1/q$ interaction in polar materials will strongly favor emission of small-q phonons. Because these phonons are most easily screened, it might be expected that high-density effects might be more readily observable. The total emission frequency is the sum of all possible transitions, weighted by the screened frequency of phonon emission at each q. For both thermalized and nonthermalized distributions, the ultimate goal of these analyses is a detailed description of the time evolution of the excited carrier distribution.

ACKNOWLEDGMENTS

It is a pleasure to thank Marshall I. Nathan for many useful discussions as well as for a critical reading of the manuscript. The author is also grateful to Peter J. Price, Robert C. Frye, William P. Dumke, James A. Van Vechten, and Marc H. Brodsky for helpful suggestions at various stages of this work. In addition, she is pleased to acknowledge an informative conversation with Arthur L. Smirl.

[1]E. J. Yoffa, Phys. Rev. B 21, 2415 (1980).

[2]R. Tsu, J. E. Baglin, T. Y. Tan, M. Y. Tsai, K. C. Park, and R. Hodgson, in *Laser-Solid Interactions and Laser Processing-1978*, edited by S. D. Ferris, H. J. Leamy, and I. M. Poate, AIP Conf. Proc. No. 50 (AIP, New York, 1979), p. 344.

[3]For a recent collection of papers on laser annealing, see *Laser and Electron Beam Processing of Materials*, edited by C. W. White and P. S. Peercy (Academic, New York, 1980).

[4]I. B. Khaibullin, E. I. Shtyrkov, M. M. Zaripov, R. M. Bayazitov, and M. F. Galjautdinov, Radiat. Eff. 36, 225 (1978).

[5]J. A. Van Vechten, R. Tsu, F. W. Saris, and D. Hoonhout, Phys. Lett. A 74, 417 (1979); J. A. Van Vechten, R. Tsu, and F. W. Saris, *ibid.* 74, 422 (1979).

[6]H. W. Lo and A. Compaan, Phys. Rev. Lett. 44, 1604 (1980).

[7]A. L. Smirl, J. R. Lindle, and S. C. Moss, Phys. Rev. B 18, 5489 (1978).

[8]A. Elci, M. O. Scully, A. L. Smirl, and J. C. Matter, Phys. Rev. B 16, 191 (1977).
[9]R. F. Leheny and J. Shah, Solid-State Electron. 21, 167 (1978).
[10]C. V. Shank, R. L. Fork, R. F. Leheny, and J. Shah, Phys. Rev. Lett. 42, 112 (1979).
[11]D. von der Linde and R. Lambrich, Phys. Rev. Lett. 42, 1090 (1979).
[12]D. H. Auston, S. McAfee, C. V. Shank, E. P. Ippen, and O. Teschke, Solid-State Electron. 21, 147 (1978).
[13]J. Shah, Phys. Rev. B 10, 3697 (1974).
[14]R. Stratton, Proc. R. Soc. London Ser. A 246, 406 (1958).
[15]R. Ulbrich, Phys. Rev. Lett. 27, 1512 (1971).
[16]J. Shah, C. Lin, R. F. Leheny, and A. E. DiGiovanni, Solid State Commun. 18, 487 (1976).
[17]R. F. Leheny, J. Shah, R. L. Fork, C. V. Shank, and A. Migus, Solid State Commun. 31, 809 (1979).
[18]J. Shah and R. C. C. Leite, Phys. Rev. Lett. 22, 1304 (1969).
[19]W. P. Latham, A. L. Smirl, and A. Elci, Solid-State Electron. 21, 159 (1978).
[20]Energy relaxation of photoexcited carriers in GaAs at lower densities, $N \sim 10^{11}$–10^{14} cm^{-3}, is discussed by R. Ulbrich, Phys. Rev. B 8, 5719 (1973).
[21]H. Ehrenreich, J. Phys. Chem. Solids 8, 130 (1959).
[22]E. J. Yoffa, Appl. Phys. Lett. 36, 37 (1980).
[23]E. J. Yoffa, J. Phys. (Paris) 41, C4-7 (1980).
[24]A. Elci, A. L. Smirl, C. Y. Leung, and M. O. Scully, Solid-State Electron. 21, 151 (1978).
[25]E. J. Yoffa, in *Laser and Electron Beam Processing of Materials*, edited by C. W. White and P. S. Peercy (Academic, New York, 1980), p. 59.
[26]D. Pines, *Elementary Excitations in Solids* (Benjamin, New York, 1964).
[27]H. Fröhlich, Proc. R. Soc. London Ser. A 160, 230 (1937).
[28]J. M. Ziman, *Electrons and Phonons* (Clarendon, Oxford, 1960).
[29]The definition of the width Γ differs slightly from that used in Ref. 1; the numerical results obtained here for Si are different for that reason.
[30]D. E. Aspnes, Phys. Rev. B 14, 5331 (1976).
[31]W. B. Joyce, Appl. Phys. Lett. 32, 680 (1978).
[32]W. B. Joyce and R. W. Dixon, Appl. Phys. Lett. 31, 355 (1977).
[33]J. A. Van Vechten, in *Laser and Electron Beam Processing of Materials*, edited by C. W. White and P. S. Peercy (Academic, New York, 1980), p. 53.
[34]W. F. Brinkman and T. M. Rice, Phys. Rev. B 7, 1508 (1973).
[35]W. Fawcett, A. D. Boardman, and S. Swain, J. Phys. Chem. Solids 31, 1963 (1970).
[36]E. A. Meneses, N. Jannuzzi, and R. C. C. Leite, Solid State Commun. 13, 245 (1973).
[37]P. Motisuke, C. A. Arguello, and R. C. C. Leite, Solid State Commun. 16, 763 (1975).
[38]J. Shah, Phys. Rev. B 9, 562 (1974).
[39]E. Lluesma, G. Mendes, C. A. Arguello, and R. C. C. Leite, Solid State Commun. 14, 1195 (1974).
[40]J. Shah, Solid-State Electron. 21, 43 (1978).
[41]H. M. van Driel, Phys. Rev. B 19, 5928 (1979).
[42]D. von der Linde, Phys. Rev. B (in press).
[43]R. C. C Leite, Solid-State Electron. 21, 177 (1978).